ELSEVIER

Journal of Chromatography A, 695 (1995) 243–257

JOURNAL OF CHROMATOGRAPHY A

Ultraviolet–visible detection for capillary gas chromatography and combined ultraviolet–mass spectrometry using a remote flow cell

Murray Hackett[a,1], Houle Wang[a], Glenn C. Miller[a], Darryl J. Bornhop[a,b,*,2]

[a]*Department of Biochemistry, University of Nevada, Reno, NV 89557, USA*

[b]*Linear Instruments Corporation, 2325 Robb Drive, Reno, NV 89523, USA*

First received 22 August 1994; revised manuscript received 1 November 1994; accepted 9 November 1994

Abstract

A scanning UV–Vis detector, linked by fiber optics to a heated remote flow cell, was interfaced to a gas chromatograph and gas chromatograph–mass spectrometer equipped with conventional split/splitless injectors and a 30 m × 0.32 mm, 0.25 μm capillary column. Gas-phase UV spectra with a 3 nm effective bandpass are shown for benzene, biphenyl, anthracene, phenanthrene, benzo-α-pyrene, methylanisoles and polychlorinated biphenyls. Chromatograms at a single wavelength are presented for Aroclors 1254 and 1221. A dual mass–UV chromatogram is shown for unleaded gasoline. Calibration curves generated for aromatic hydrocarbons suggest linearity of detector response over a range of about 10^4. A total absorbance chromatogram is shown for four components of a test mixture. Detection limits for a moderate UV absorber, biphenyl, were 1.0 ng in summed scanning mode and 750 pg in single-wavelength mode, using a criterion of three standard deviations of the baseline noise. The single-wavelength detection limit for naphthalene, a stronger UV absorber, was 90 pg.

1. Introduction

Since the first paper by Kaye [1] published in 1962, there have been less than twenty papers published in the open literature dealing with UV detection schemes for gas chromatography, exclusive of photoionization detectors. Given the ubiquitous nature of UV–Vis spectrophotometers and UV HPLC detectors, it seems somewhat anomalous that UV detection for GC has not attracted more attention.

Previous work has included packed-column GC with combined absorbance and fluorescence detection [2,3], capillary GC with single-wavelength UV detection [4], and packed-column GC with modified commercial photodiode array LC detectors [5–7]. Russian- and Chinese-language papers have also described combined GC–UV [8,9]. More recently, GC–UV spectra of chlorobenzene isomers have been published [10]. The details of our initial hardware design, with emphasis on the cooling requirements, flow cell temperature stability, optics, and a review of previous work (up to 1991) have been presented

* Corresponding author.

[1] Present address: Departments of Chemistry and Pathology, University of Virginia, Charlottesville, VA 22901, USA.

[2] Present address: Department of Chemistry and Biochemistry, Texas Tech. University, Lubbock, TX 79409, USA.

0021-9673/95/$09.50
SSDI 0021-9673(94)01105-2

elsewhere [11] and will only be briefly summarized. Here we report improved flow cells and demonstrate their application with chromatograms, spectra, calibration data and detection limits. We also discuss the instrumentation in terms of its operating characteristics, analyte specificity and how the technique may be improved in the future.

This UV detection scheme collected "on the fly" full-scan (192–360 nm) spectra or single-wavelength chromatograms from capillary GC peaks. The non-destructive nature of GC–UV lends itself to hyphenated techniques, in which the heated exit line of the GC–UV flow cell can serve as the inlet for another detector, such as a flame ionization detector, mass spectrometer, electron-capture detector or Fourier transform (FT) infrared spectrometer. In this report we describe an instrument that consisted of a quadrupole mass spectrometer with a gas-phase UV detector built into the transfer line between the gas chromatograph and the ion source. This arrangement allowed collection of simultaneous gas-phase UV spectra and 70 eV positive ion electron impact mass spectra.

2. Description of instrumentation

2.1. GC–UV flow cells and remote detector

All data were collected using one or the other of two prototype GC–UV systems, which were based on somewhat different flow cells. However, the dimensions of the illuminated portions were the same. The earlier design, similar to that reported in [11], consisted of a heated, gold-plated, stainless-steel flow cell of "Z" type configuration [12] with an illuminated volume of approximately 85 μl and a pathlength of 12 mm. The body was surrounded by an aluminum heat sink which contained cooling passages, the sample and reference photodetectors (Hamamatsu S1226-8BQ, Bridgewater, NJ, USA), and associated current-to-voltage conversion electronics. Remote operation was accomplished by connecting the photodetectors to a commercial UV detector (Model 206HR; Linear Instruments, Reno, NV, USA) with a heat-stable, fiber optic beam splitter [11,13]. The 3 mm O.D. fiber optic bundle was assembled using polyimide-based high-temperature adhesives (High Light Fiber Optics, Caldwell, ID, USA). The scanning monochromator, forward optical bench design of the detector did not require the sample cell to be placed directly in a straight-line configuration between the monochromator and photodetectors, thus lending itself to use with a heated, remote flow cell. This, in turn, allowed physical separation of the high-heat and room temperature portions of the system. The remote flow cell approach would not have been feasible using any existing diode array-based detector. Diode array designs reported in the open literature [6,7] have been restricted to flow cell temperatures at or below 150°C, which limits applicability of the device to molecules with significant vapor pressures at this temperature.

The most significant barrier to the development of GC–UV has been control of thermal noise. At temperatures required for GC work, noise from black body radiation was a significant problem [11]. This difficulty was overcome by cooling the photodetectors and associated electronics while still keeping them in close proximity to the heated portion of the flow cell. This configuration also minimized the number of elements in the optical train, thus keeping light loss to a minimum. Using photoelements designed specifically to have low response in the IR region allowed us to generate noise and drift values comparable to those for similar equipment used for HPLC detection at room temperature, measured at 254 nm in the scanning mode: $2 \cdot 10^{-5}$ AU short-term noise and $1 \cdot 10^{-4}$ AU/h drift with a flow cell temperature of 350°C. The sample light levels were ratioed with the reference beam intensity to minimize drift associated with lamp instabilities and other factors independent of the actual sample absorbance. The system had an effective bandpass of about 3 nm.

The most recent flow cell design, utilized to construct the tandem GC–UV–MS instrument, used the "U-cell" configuration [4], shown in Fig. 1. This design allowed easier manipulation of the inlet and exit lines, and the dead volume was smaller by several μl. As with the Z-cell, all contact surfaces were gold plated to minimize

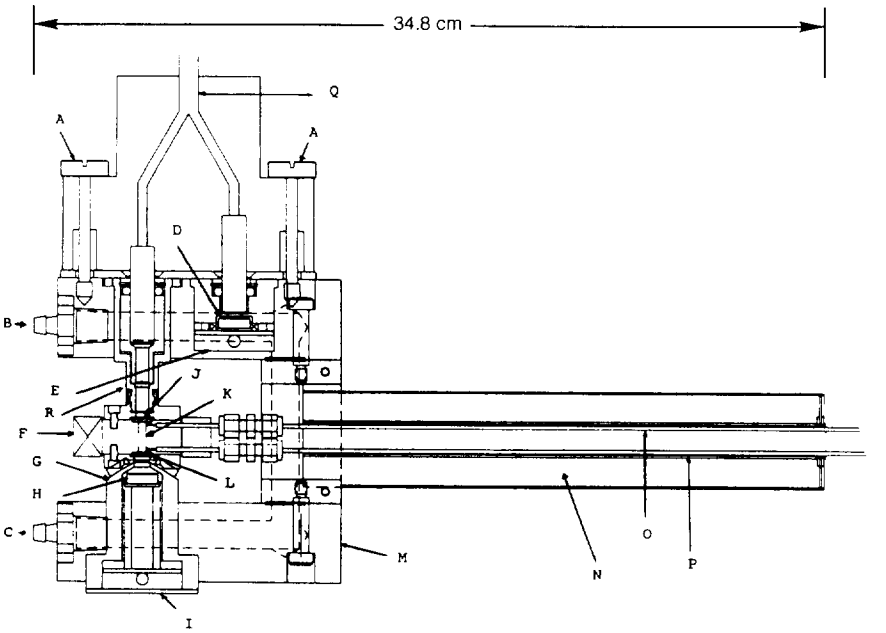

Fig. 1. Line drawing of the "U" flow cell. A = Thumb screws, beam splitter; B = coolant inlet; C = coolant outlet; D = reference photodiode; E = reference preamplifier; F = band heater; G = IR photon "hood"; H = sample photodiode; I = sample preamplifier; J = sapphire window with gaskets; K = flow cell, 12mm × 3 mm; L = sapphire window with gaskets; M = aluminum heat sink; N = transfer line heater; O = sample inlet line; P = sample exit line; Q = fiber optic beam splitter; R = lens.

analyte degradation (Hammon Metal Plating, Palo Alto, CA, USA). A cold shield, consisting of an aluminum cone-shaped hood (see Fig. 1) was introduced between the heated region of the cell and the sample photodetector to physically block IR photons from the cell's periphery from striking the photoelement. This was done without vignetting rays of interest.

The cooling system for both cells consisted of a standard recirculating chiller (Model 1165; VWR Scientific, San Francisco, CA, USA) using water–ethylene glycol (50:50) at 15°C.

The Z-cell was connected, through a heated transfer line, to a GC system (5830A; Hewlett-Packard, Avondale, PA, USA) modified for split/splitless capillary operation (J & W, Rancho Cordova, CA, USA). The separate transfer line [14] was constructed of 1 m of thin-wall 1.59 mm O.D. stainless-steel tubing, Swagelok end fittings, heat tape and glass wool. Heat was controlled by a simple Variac. The capillary column was inserted through the transfer line directly into the flow cell in a manner similar to a direct insertion GC–MS interface.

2.2. Flow cell optical design considerations

The critical parameters were the pathlength, refractive index perturbations, scattering, light throughput, and flow cell volume. It was important to maximize the absorbance pathlength for Beer's law considerations, while minimizing the effective flow cell volume for separation performance [12]. This was accomplished by using optical design software (Beam 4; Stellar Software, Berkeley, CA, USA) running on an MS-DOS computer. Using a fixed pathlength of 12 mm and a diameter of 3 mm, we first constructed an optical train based on constraints including: (1) the positions of the sapphire flow cell windows; (2) the minimum diameter of the cell; (3) the window and active surface area of the photodetector; and (4) the fiber optic used to launch the excitation light (Figs. 1 and 2). Once

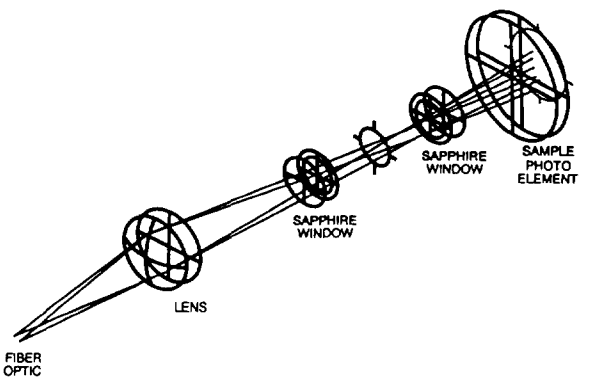

Fig. 2. Flow cell optics, showing the simulated paths of two rays of light at 210 nm.

the major components were chosen, a set of rays was defined by wavelength, position along the optical path, and divergence. Wavelengths were chosen based on typical UV–Vis absorbance applications, we used 210, 254 and 546 nm. The fiber optic employed a high density quartz bundle. Ignoring packing losses, we assumed the bundle would produce a diverging beam of uniform intensity and predictable diameter. A quantitative measure of beam diversion was obtained based on the numerical aperture of the fiber optic, 0.22, and defined the angle from normal that the rays traversed as they exited the bundle. Fig. 2 shows only two sets of rays for clarity. These two sets of rays originate from the edge of the fiber optic and the center, respectively. After evaluation of several optical elements, it was found that the beam could be effectively focused with a single plano-convex lens (JLM Optical, Rochester, NY, USA). This lens was chosen to be an achromatic singlet with an effective focal length, at 546 nm, of 11 mm. Through iterative calculations the position of the focusing lens was determined such that light throughput was maximized and scattering effects due to wall interactions were minimized. For the 210 nm light traced in Fig. 2, the focus is 3.9 mm from the end window of the cell. The paraaxial focus of light is wavelength dependent, therefore optical analyses at 254 and 546 nm were also performed. With proper placement of the lens (Figs. 1 and 2) it was found that the beam focus remained within the flow cell across the UV (180–400 nm) and into the visible (to 700 nm).

Design investigations were performed to evaluate the use of a second lens to capture and focus the rays that exit the flow cell. The normal losses expected due to the addition of an extra optical component outweighed the advantage of collecting marginal rays.

With all optical components defined, additional ray tracing analysis was performed. This was accomplished by running a number of random ray calculations at various wavelengths. These rays were launched from the fiber optic, traced through the optical train and quantified as a percentage of rays launched versus rays collected. It was found that under the worst-case scenario 80% of all rays launched traversed the flow cell and hit the photocell active surface. Further, it was observed that at 210 and 254 nm very few rays struck the wall of the flow cell or were scattered out of the optical path.

2.3. GC–UV–MS

For these experiments the U-cell prototype was used, which was constructed with an integrated heated transfer line (1.59 mm O.D. thin-wall stainless-steel tubing) that contained both entrance and exit lines (Fig. 1). This device was placed on a stand constructed of plywood and particle board at the back of the GC–MS system transfer line oven (Finnigan MAT Model 4023, San Jose, CA, USA). A hole in the GC–MS transfer line oven, originally designed for a jet separator used for packed columns, accommodated the flow cell transfer line in a 90° configuration relative to the MS transfer line oven. The hole had to be enlarged by 3 mm with a file and tin snips. The GC column entered the transfer line oven through a hole in the top of the GC oven (Finnigan MAT Model 9610), as for the normal capillary GC–MS arrangement. The end 20 cm or so was carefully bent to 90° and inserted into the flow cell/transfer line assembly until resistance was felt. A 60 cm length of 0.53 mm I.D. deactivated fused-silica tubing (Supelco, Bellefonte, PA, USA) was used for the

exit line of the U-cell, and was inserted directly into the ion source block of the mass spectrometer. Swagelok end fittings with Vespel ferrules (Supelco) for the inlet/exit lines and high-temperature polyimide gaskets for the two flow cell sapphire windows [11] provided gas-tight seals. The 206 detector, and the box containing the flow cell/transfer line heating controller and 24 V d.c. power supply, were placed on shelves constructed approximately 18 cm above and slightly to the left of the gas chromatograph. The heating controller (Watlow Series 408, St. Louis, MO, USA) was of design similar to that used in the Z-cell prototype, but used 24 V d.c. instead of 120 V a.c. to drive two matched heating elements instead of just the band heater (Watlow Model B1EOLA1) on the flow cell proper. The transfer line was eliminated as a separately controlled heated zone.

2.4. Data systems

The UV detector was controlled by a microcomputer (Model PS2 55 SX; IBM, San Jose, CA, USA) running Windows-based (Microsoft, Redmond, WA, USA) data acquisition software, originally designed for conventional analytical-scale HPLC (206 software, Linear Instruments). Although intended for use with peaks requiring somewhat slower time constants, this software worked well for all but the fastest peaks eluting from a 0.32 mm capillary GC column, with minimal peak distortion when the shortest rise time filter was used, 0.1 s. The rise time control was based on a second-order Bessel filter, encoded in firmware within the 206, that served the same purpose as the traditional resistance–capacitance (RC) filter [15] used in chromatography to avoid recording events, e.g. high-frequency noise, occurring with a faster time constant than those of interest. The rise time filter was set to a value of twice the desired RC time constant to achieve similar results [13], no more than one third the FWHH (full width at half height) peak width. Mass spectral data were collected with a standard Finnigan INCOS data system running on a Nova 4C computer.

3. Experimental

3.1. Reagents

Benzene (Burdick & Jackson, Muskegon, MI, USA), hexane, toluene and methanol (Fisher, Fair Lawn, NJ, USA) were HPLC grade and used as received. Anthracene, 2-methylanisole, 3-methylanisole, 4-methylanisole, nitrobenzene, 1,2,4,5-tetramethylbenzene, *o*-xylene, *m*-xylene, *p*-xylene (Aldrich, Milwaukee, WI, USA), phenanthrene (J.T. Baker, Phillipsburg, NJ, USA), coumarin (U.S. Biochemicals, Cleveland, OH, USA) and benzo-α-pyrene (Sigma, St. Louis, MO, USA) were used as received. Biphenyl was recrystallized in our laboratory from a technical-grade product. Aroclors 1221 and 1254 (Monsanto, St. Louis, MO, USA) were technical formulations used as received. 1,1-Dichloro-2,2-bis(*p*-methoxyphenyl)ethene (DMDE) was synthesized from the dehydrohalogenation of 1,1,1-trichloro-2,2-bis(*p*-methoxyphenyl)ethane (methoxychlor). Methyl parathion was recrystallized from a technical formulation (Pennwalt, Monrovia, CA, USA). All chemicals used in this study were checked for identity and purity using MS and condensed-phase UV–Vis spectrophotometry.

3.2. Conditions

Chromatographic conditions used with the GC–UV, GC–MS and GC–UV–MS instruments were the same: Grob-type splitless injection at 300°C, 1 min delay, 1 m × 0.32 mm retention gap; program, 30°C hold 2 min, 30–60°C at 20°C/min, 60–280°C at 5°C/min; helium carrier at 68.9 kPa head pressure, 30 cm/s linear velocity at 200°C for the Z-cell GC–UV system, as determined by methane injection with a flame ionization detector in place of the UV flow cell; linear velocity varied slightly ($< 10\%$) for the GC–MS and GC–UV–MS; temperatures were MS source 270°C, MS vacuum manifold 100°C, transfer lines 300°C, UV flow cells 300°C, unless otherwise indicated. The column used for all data reported in this paper was a 0.32 mm × 30

meter, 0.25 μm stationary phase thickness DB5 (J & W).

3.3. Chromatographic efficiency

Absolute retention times divided by peak widths at FWHH, t_R/w_H, were calculated for the Z-cell GC–UV system, GC–MS, and combined U-cell GC–UV–MS. We report the data shown in Table 1 in this manner so as to avoid the requirement for isothermal conditions implied by the various expressions used for theoretical plate calculations. Each component of the test mix shown in Table 1 was present at a concentration of 100 ng/μl in hexane, 1.0 μl was injected. Rather than try to match linear velocities exactly, each GC system was individually optimized in terms of carrier gas flow-rate to reach the highest efficiency consistent with the UV scanning speed limitation discussed below in Sections 3.5 and 4.3. Each instrument configuration was operated under the same temperature regimen. Calculations for the GC–MS and GC–UV–MS were made with RIC (reconstructed ion current) data.

3.4. Condensed-phase spectrophotometry

A DU-70 UV–Vis scanning spectrophotometer (Beckman Instruments, Fullerton, CA, USA), with an effective bandpass of 2 nm, was used as described above for checking the purity of reagents. It was also used to generate the condensed-phase spectra of biphenyl in hexane (see Fig. 5), and the molar absorptivities in Table 2. The instrument was scanned from 190 to 360 nm. For the molar absorptivity calculations, single-wavelength mode was used at λ_{max} for each compound, and the log ϵ values calculated from the Beer–Lambert Law [16].

3.5. Scanning parameters and signal processing for GC–UV

The detector was scanned in the UV mode from 192 to 360 nm with a 2-nm step over a period of approximately 1.0 s at a fixed sampling rate of 96 points/s, with the exception of anthracene, which was scanned from 200 to 380 nm. After the raw data were acquired, the files were transferred to another DOS personal computer running Sigmaplot software (Jandel Scientific, Sausalito, CA, USA), which was used to plot all optical spectra and chromatograms. All gas-phase spectra were smoothed using the binomial three-point method given by Bevington [17]. To facilitate off-line data transfers and to integrate chromatographic peaks for the biphenyl calibration data, it was necessary to write two short programs in the C computer language (Borland Turbo C, Scotts Valley, CA, USA). The peak

Table 1
t_R/w_H Values for test mix using GC–MS, GC–UV and GC–UV–MS

Compound[a]	RRT[b]	t_R/w_H		
		GC–MS	GC–UV	GC–UV–MS
Benzene	1.00	Solvent front	102	Solvent front
Toluene	1.49	106	91	Solvent front
Nitrobenzene	4.61	183	169	182
1,2,4,5-TMB	4.93	198	194	201
Naphthalene	5.58	232	218	173
Coumarin	7.90	272	272	253
MP	9.50	686	404	467
DMDE	11.31	666	513	533

Numbers given are means from three replicate determinations. All retention times had R.S.D. values of $<2\%$.
[a] TMB = Tetramethylbenzene; MP = methyl parathion; DMDE = 1,1-dichloro-2,2-bis(*p*-methoxyphenyl)ethene.
[b] Relative retention on the GC–UV system.

Table 2
Condensed-phase log ϵ values and GC–UV single-wavelength detection limits at λ_{max}

Compound	λ_{max} (hexane) (nm)	log ϵ	λ_{max} (GC–UV) (nm)	MDL (pg)
Benzene	204	3.90	194	1300
Toluene	206	3.86	192[a]	5500
Naphthalene	221	5.06	211	90
Biphenyl	202	4.66	195	750
Anthracene	252	5.34	236	40

Analytes were injected in amounts expected to yield *S/N* of 5:1 and detection limits (minimum level of detection, MDL) were calculated as discussed in the text. Numbers given are means from three replicates, R.S.D. values were $<5\%$.
[a] Shoulder or end absorbance.

integration was based on a simple summation algorithm. Calibration statistics were generated with Mathcad software (MathSoft, Cambridge, MA, USA) running on an MS-DOS computer, using weighted versions of the regression equations given by Miller and Miller [18]. To create the TAC (total absorbance chromatogram) of the test mix (Table 1), shown in Fig. 9, a third C program was written. The TAC plot was analogous to an RIC plot in GC–MS or a Gram–Schmidt vector orthogonalization in GC–FT-IR; the program summed all wavelengths over each scan. The C source code is available from the authors, and has been published in a doctoral dissertation [19].

3.6. Preparation of environmental samples

Drums (55 gallons) of unknown liquids were sampled by hand with the aid of a small pump into glass jars sized to hold about 50 ml of sample. A few μl were removed in the laboratory, diluted 10 to 100 × with hexane, with 1 μl injected into the GC–UV–MS instrument.

4. Results and discussion

4.1. Spectral quality

The gas-phase UV spectra of four aromatic compounds, shown in Figs. 3 and 4, illustrate the analyte specificity inherent in the method. Note the fine structure characteristic of the *B* band, a forbidden transition [16], in the gas-phase spectrum of benzene in Fig. 4. Although broadened, as expected [20], fine structure for benzene absorbance was still seen at 275°C. The expected band broadening and decrease in molar absorptivity with increasing transfer line/flow cell temperature [20,21] have been observed to occur for benzene (Fig. 4) and toluene (data not shown) when analyzed over a range of temperatures from 50 to 350°C. All four compounds shown in Figs. 3 and 4 yielded spectra which were manually searched against data bases of condensed-phase spectra acquired using non-polar solvents. For instruments of similar resolution, GC–UV spectral features tend to be broadened and hypsochromically shifted when compared with those observed in the condensed phase. The band narrowing effects expected due to the absence of solvent seemed to be balanced by the thermal band broadening effects, such that the net result of these opposing forces were spectra which were similar to those acquired in non-polar liquids. Comparisons between condensed-phase and GC–UV gas-phase spectra are expected to become more complex when polar solvents, analytes capable of forming hydrogen bonds, etc. are used. The incorporation of a supersonic jet expansion, as has been accomplished for UV fluorescence detection combined with GC [22], would serve to narrow spectral bands in gas-phase absorption measurements. However, in its present state of development, this modification would add additional mechani-

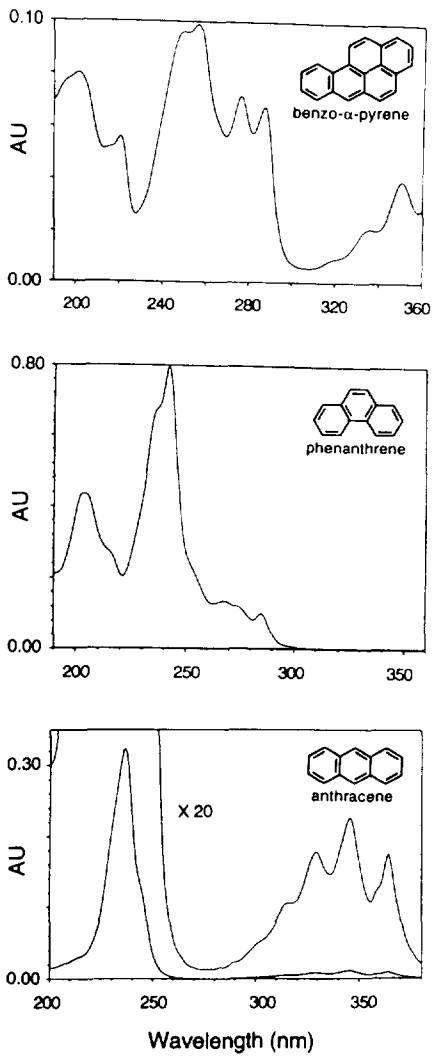

Fig. 3. Spectra of aromatic hydrocarbons acquired in the gas phase using the Z-cell GC–UV instrument. The flow cell was heated to 280°C.

cal complexity and potential sources of non-linear response.

In Fig. 5, a spectrum of biphenyl in hexane, at room temperature, is compared with a spectrum acquired from a GC peak at 300°C. They are similar, with the exception that the primary and secondary bands are slightly blue shifted in the gas phase relative to condensed-phase measurements.

UV spectra have long been known to show significant differences among closely related isomers [16]. This was illustrated by comparing the GC–UV spectra of 100 ng each of *ortho*-, *meta*- and *para*-substituted methylanisoles (Fig. 6). The mass spectra of methylanisoles acquired with the GC–UV–MS instrument (data not shown), M_r 122, differed slightly in the relative abundances of fragment ions at m/z 91 and 107; otherwise they were the same, and similar to library spectra. This difference was more pronounced between the *meta*- and the *ortho*-/*para*-substituted isomers, but it was not possible to distinguish the *ortho*/*para* isomers from one another. The *para*/*meta* isomers also coeluted under our GC conditions. The UV spectrum of each isomer was sufficiently different due to shifting in the *K* band region to allow unambiguous identification.

Polychlorinated biphenyls (PCBs) are complex mixtures of closely related isomers, which have been of environmental interest. Spectra for the four largest peaks in the GC–UV chromatogram of Aroclor 1221 (Fig. 7A), are superimposed and plotted in Fig. 7B. All four peaks were readily differentiated based on the *K* band region in their absorbance spectra [16], without recourse to taking first or second derivatives. Aroclor 1221 is a technical formulation of PCBs consisting primarily of isomers substituted with one and two chlorines [23]. Additional chlorination was expected to yield broader, more diffuse absorbance bands [24]. This was observed in spectra (not shown) taken from the GC–UV chromatogram of Aroclor 1254, shown in Fig. 8, a material which consists primarily of four, five and six chlorine-substituted isomers [23]. Positive identification would, in this case, still rely heavily on retention time. The single-wavelength chromatograms shown in Figs. 7A and 8 are analogous to an extracted ion profile in GC–MS, in that they were extracted from full-scan data.

Results to date suggest the spectra for compounds presented in this paper are reproducible, within the specifications published for the unmodified LC detector [13], over a broad range of flow cell temperatures, flow-rates, and GC temperature programs (accuracy ± 1 nm, precision better than 0.01 nm). As with ion relative abun-

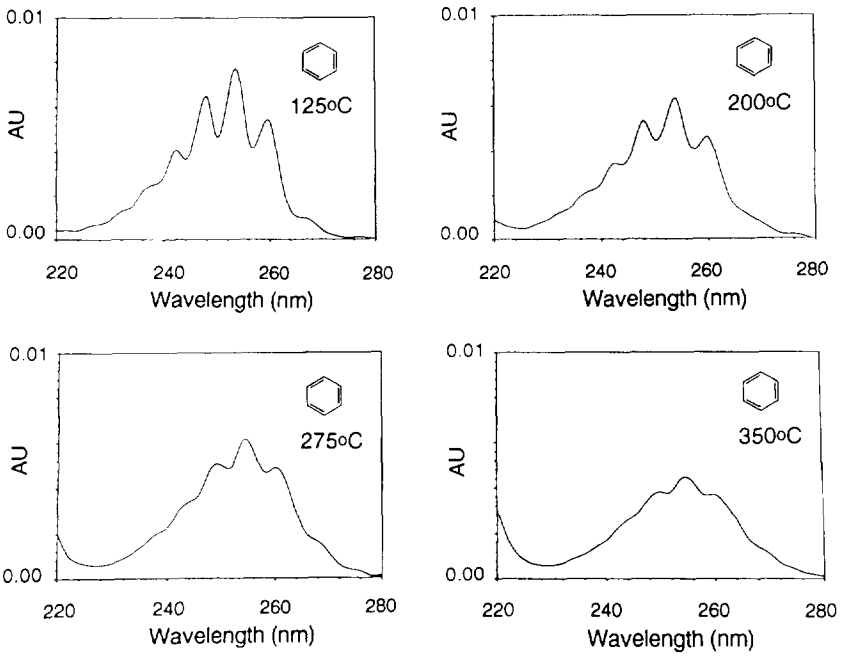

Fig. 4. Fine structure region of the GC–UV spectrum of benzene at four flow cell temperatures.

dance measurements in GC–MS, the least spectral distortion was observed with spectra taken from the center of the GC peaks.

4.2. Linearity of detector response and detection limits

A standard curve for biphenyl was linear over a range of about 10^4. These data were acquired using the Z-cell. The linear regression calculations were weighted by the inverse S.D. for the three replicates at each concentration such that the lowest concentrations would have the strongest influence on the coefficients: $R^2 = 0.994$, slope $= 5.62 \cdot 10^{-5}$ AU min μl/ng, intercept $= -1.8 \cdot 10^{-6}$ AU min, $n = 18$ observations at 6 concentrations, S.D. (of the y-residuals) $= 6.6 \cdot 10^{-6}$ AU min, S.D.$_{\text{slope}} = 5.9 \cdot 10^{-7}$ AU min μl/ng, S.D.$_{\text{int}} = 6.4 \cdot 10^{-7}$ AU min. Chromatographic band broadening became significant ($> 10\%$) above 500 ng/μl, but peak area remained linear up to 2.0 μg/μl. This calibration curve was based on absolute detector response, in the single-wavelength mode at 200 nm, without the use of an internal standard. Similar linear responses were observed with more polar materials, coumarin [11] and underivatized phenols, e.g. pentachlorophenol. We attribute these results to the absence of solvent effects in the gas phase. Calibration curves plotted for benzene and toluene were limited to a linear dynamic range of about 10^3 due to their low molar absorptivities. Good linearity was also observed when biphenyl calibration data, acquired using full-scan mode, were plotted both as abstracted single-wavelength chromatograms and as TACs. Using the TAC chromatogram improved biphenyl detection limits by a factor of 6, when compared to the single-wavelength chromatogram at 200 nm abstracted from full-scan data, giving a value of 1.0 ng at three times the standard deviation of the baseline noise, 3 S.D.$_n$ [25]. Fig. 9 shows the S/N improvement observed when a TAC of the relevant wavelengths was compared with a single-wavelength chromatogram for the test mix (Table 1). Improvement in S/N was compound dependent, and fell in the range of 4 to 8×. For sake of clarity, only the early eluters are shown in Fig. 9.

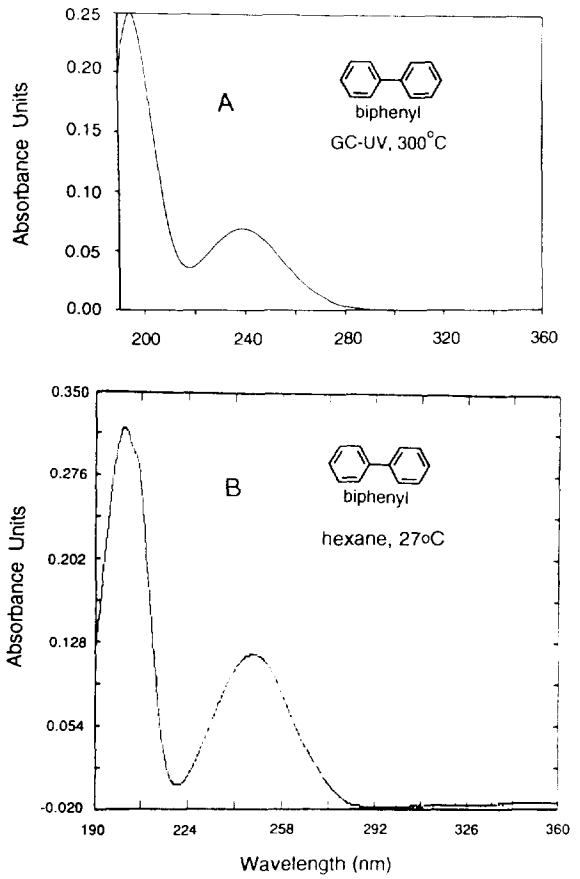

Fig. 5. Biphenyl spectra acquired in the vapor phase with 100 ng injected into the GC–UV system (A), and in the condensed phase at room temperature (B).

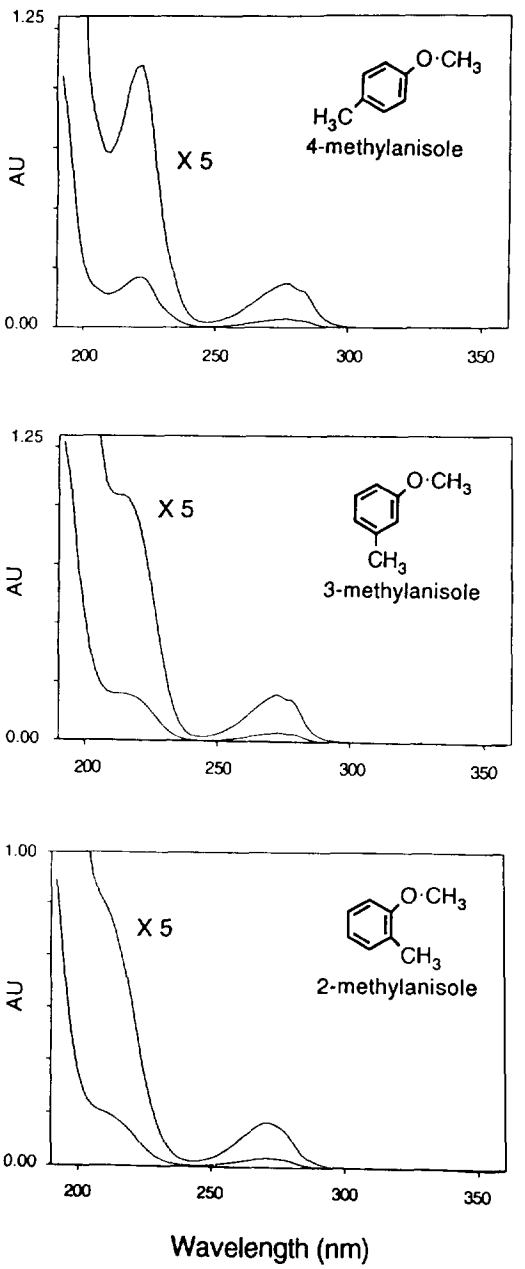

Fig. 6. GC–UV time-slice spectra collected for 100 ng each of methylanisole isomers. The flow cell temperature was 250°C.

TACs were not displayed in "real time" during data collection and had to be generated post-run.

Observed detection limits, based on a criteria of 3 S.D.$_n$, were directly proportional to molar absorptivity. The condensed-phase log ϵ values, for five analytes and their single-wavelength GC–UV detection limits, are shown in Table 2. No attempt has been made to account for injector efficiency, temperature programming or other environmental influences which might arise under different conditions. Deviations from the Beer–Lambert law have not been observed to date, within the mass loading limits imposed by the DB5 capillary column employed for sample introduction. More work needs to be done to examine the roles of flow cell temperature, GC oven programming, and scanning parameters on

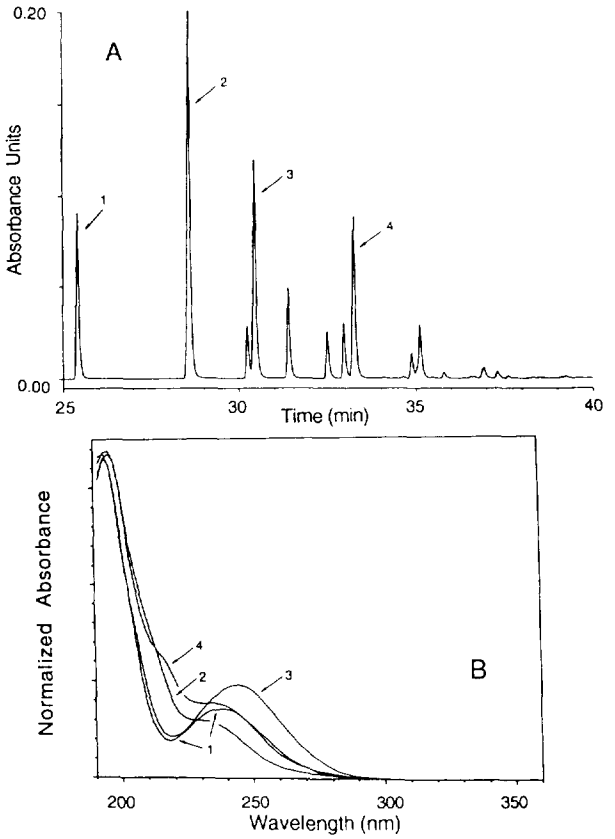

Fig. 7. Arochlor 1221, 1 μg/μl in hexane, 1-μl injection, single-wavelength (200 nm) chromatogram (A), and four time-slice spectra representing the peaks indicated are superimposed (B) after being normalized to the same relative intensity.

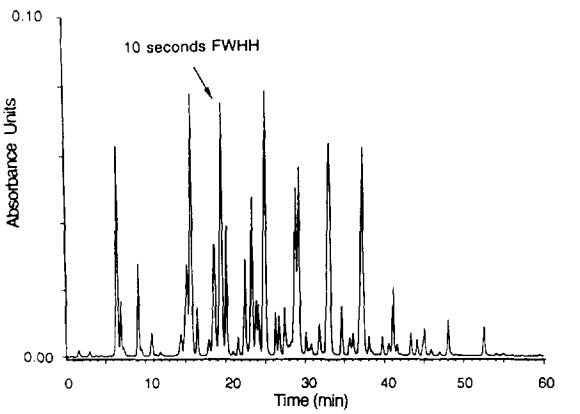

Fig. 8. Single wavelength (220 nm), Arochlor 1254, 1 μg/μl in hexane, 1-μl injection, acquired as described under *Conditions*, with the exception that a 1°C/min ramp was used in order to resolve as many peaks as possible.

detector response before a definitive statement can be made as to its suitability for quantitative GC work.

4.3. Extracolumn band broadening and chromatographic performance

Because of the flow cell volume employed, it was anticipated that some peak broadening would be observed, relative to a chromatographic system optimized for use with the mass spectrometer alone. However, the loss in chromatographic efficiency introduced by the use of the U-cell in series with the mass spectrometer was small, about 10%. Table 1 shows a comparison of t_R/w_H values [26] measured with the Z-cell GC–UV system, GC–MS and GC–UV–MS. The results for the combined GC–UV–MS U-cell-based system differed only slightly from those for the Z-cell GC–UV. Both systems showed a significant loss in efficiency for the two highest boilers, methyl parathion and DMDE, when compared to the GC–MS without the UV flow cell. This same difference in performance for higher boilers was also observed when the GC, normally used with the Z-cell, was used with a capillary optimized flame ionization detector instead. Such differences were not unexpected when comparing results from systems, such as those described here, with split/splitless injectors of different design [27]. This efficiency comparison also ignored the influence of vacuum on the column exit of the GC–MS. The hexane solvent front was 30% wider with the GC–UV–MS when compared to the unmodified GC–MS, such that benzene and toluene peaks were obscured in the RIC trace. This was probably due to vacuum effects within the flow cell/exit line. This vacuum was observed to be significant, in that slight leaks in the polyimide flow cell gaskets led to higher pressures ($5 \cdot 10^{-5}$ Torr; 1 Torr = 133.322 Pa) in the mass analyzer. When the leaks were repaired, the vacuum returned to normal values ($8 \cdot 10^{-7}$ Torr). The data in Table 1 are

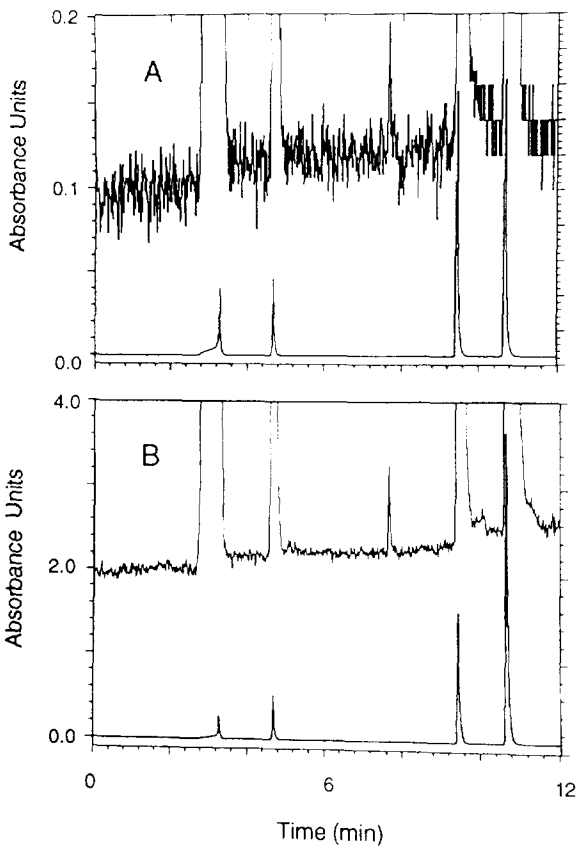

Fig. 9. Full-scan data collected for 1 μl of test mix, showing the elution of the first four components, benzene, toluene, nitrobenzene and 1,2,4,5-tetramethylbenzene. Single-wavelength (200 nm) chromatogram (A) and TAC (total absorbance chromatogram) summed over the relevant wavelengths (192–220 nm, B). Upper traces show 200 × magnification of the baseline. The small peak was an impurity.

intended to demonstrate how the GC–UV instrument compared with an established technique, in terms of chromatographic efficiency, rather than to stress the absolute magnitude of the reported values. The best overall results with scanning UV detection, and apparent sensitivity, were achieved when the helium carrier gas flow-rate was slightly lower than that of an optimization based purely on minimizing the height equivalent to a theoretical plate (HETP) or similar metric. This was at least in part due to the requirements of the data system, which had a fixed data collection rate of 96 points/s. This collection rate is slow for capillary GC, particularly when scanning over the 85 intervals required for a 190–360 nm scan incremented every 2 nm. A capillary peak, e.g. the peak indicated in Fig. 8, which is 10 s wide FWHH, is sampled 11 times at a given wavelength. This sampling rate was adequate for generating spectra and TAC plots in most cases. Because of this limitation, the system was not reliable for peaks faster than about 4 s FWHH, using the scanning parameters and data collection electronics employed in this study. One could, however, increase the number of samples/peak by choosing a larger scanning increment, e.g. 4 or 6 nm. In practice, the sampling rate became an issue when 0.32 mm columns were used at carrier flow-rates higher than those used for data reported here. To adequately determine to what extent the 85-μl flow cell volume contributes to band broadening with 0.32 mm columns, more work needs to be done with the flow cell exit line at atmospheric pressure, and the scanning speed limitation removed. Single-wavelength detection would be one option.

The introduction of a make-up flow of 2–5 ml/min of helium through a coaxial tee fitting, at the point where the transfer line joins the flow cell, resulted in a 10% gain in chromatographic efficiency. However, this increased flow-rate resulted in an approximately 50% loss in apparent sensitivity for early eluters, benzene and toluene, contained in the test mix described in Table 1. Later-eluting peaks, i.e. those with higher capacity factors, were also affected, but not as severely. The sensitivity reduction was probably caused by a combination of two factors. This is a concentration-sensitive, as opposed to a mass-sensitive, detector. Increasing the gas flow at the detector reduced the concentration of analyte present during any one time slice of the peak volume. By increasing dC/dt (rate of change in concentration with respect to time) and thus narrowing the earliest peaks to a point approaching the maximum efficiency of the column, they became too "fast" for the data system. At 2 s FWHH a peak might be sampled only

three or four times in scanning mode, with a 2-nm increment, and thus artificially truncated. Further experimentation with make-up flows for columns of 0.32 mm I.D. or larger was abandoned. Experimentation with capillary columns of smaller I.D. than 0.32 mm has not been performed in our laboratory, but has been attempted by others [28]. Due to the relatively large volume of the flow cell, it was anticipated that it would not be applicable to GC columns with an I.D. of less than 0.30 mm, or to "fast" GC.

Six repeated 1.0-μl manual injections of the standard test mix (Table 1) using the Z-cell instrument yielded an R.S.D. of 5% for peak areas. The use of an autosampler would likely give better repeatability.

4.4. Application to environmental samples

About 100 samples of organic liquids from hazardous waste sites in the western USA have been analyzed qualitatively using the U-cell-based GC–UV–MS system, with emphasis on BTX (benzene, toluene, xylenes). Most of these unknowns came from unmarked drums of technical-grade products derived from petroleum. The gas-phase UV data were especially helpful with respect to identifying signals for aromatic compounds of regulatory interest that were "buried" under signals from much higher concentrations of aliphatic compounds, rendering the MS data useful primarily for the aliphatics. This point is illustrated by a representative GC–UV–MS chromatogram of unleaded gasoline, Fig. 10. The BTX peaks were confirmed by comparing their time-slice UV spectra and retention times with those from standards run under the same conditions. Benzene and toluene were readily identified in the unknowns based on UV spectra alone. However, the time-slice GC–UV spectra of the xylene isomers were identical and similar to condensed-phase spectra, below 230 nm. The xylenes lacked sufficient S/N in the weak B band region, at higher wavelength, to discern any isomer specific fine structure. Subtle differences among xylene isomers have been observed in condensed-phase spectra, acquired using isooctane solvent [29].

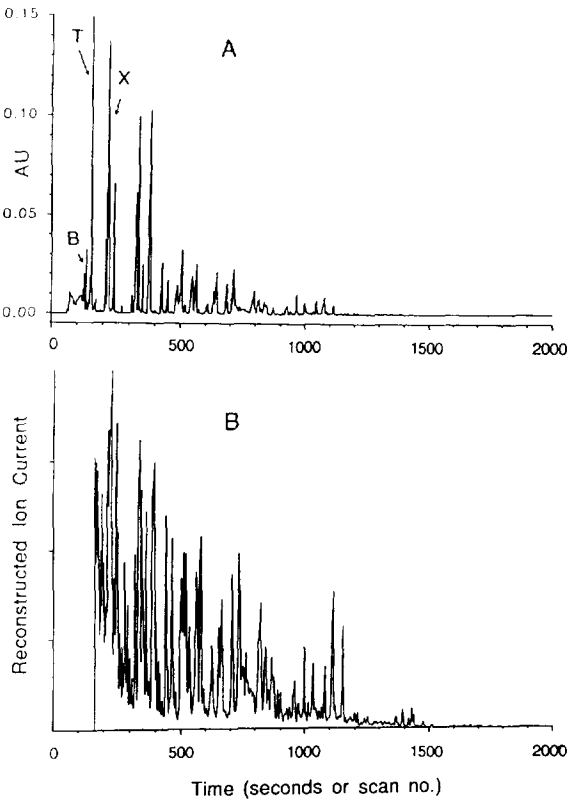

Fig. 10. GC–UV–MS dual chromatogram of unleaded gasoline diluted 1:20 with hexane, 1-μl injection. UV flow cell 250°C, order of elution for the BTX fraction (A, 200 nm) was benzene, toluene, *m*-xylene, *p*-xylene, *o*-xylene. MS data (B) were summed from m/z 50 to 550, 1 scan/s, ion source and transfer lines 250°C.

5. Conclusions

The Z-cell and U-cell GC–UV instruments were used successfully as specific detectors for aromatic compounds, which could also provide gas-phase spectral data for qualitative organic analysis. The detection hardware for the technique was relatively uncomplicated, both with respect to its construction and its application.

Molar absorptivities for transitions in the near UV are higher than those in the IR, making the UV method inherently capable of lower detection limits, for moderate to strong UV absorbers ($\epsilon > 10\,000$). The detection limits achievable for biphenyl, a representative analyte for full-scan and single-wavelength GC–UV, were reasonable for practical application (see Table 2 and discussion above) but would have to be improved, by at least two orders of magnitude, to compete with other sensitive detection methods, e.g. MS.

Calculating the TAC in the acquisition software, in real time, is an obvious improvement that would eliminate the need for much tedious off-line data processing. The TAC improved detection limits for full-scan data and would be a more informative way of observing the UV chromatograms in real time, as opposed to monitoring a single wavelength.

Our implementation of GC–UV was limited to compounds which absorb light above 190 nm. Kaye [1] demonstrated the possibility of extending a GC–UV instrument into the middle UV region, where $n \rightarrow \sigma^*$ and end absorbance from $\sigma \rightarrow \sigma^*$ transitions are observed, but common GC carrier gases are transparent. Extending the lower scanning limit of the GC–UV system from 190 to 160 nm would widen the applicability of the instrumentation to that of a non-destructive, universal detector for volatile organics.

Acknowledgements

We acknowledge engineering support provided by Louis Hlousek, Rick Mikulski and Ray Bryan. Scot Weinberger and John Wangsgaard are acknowledged for valuable discussions. Support for this work by Linear Instruments (now a part of Spectra-Physics Analytical, a division of Thermo Separation Products) and the University of Nevada is gratefully acknowledged. We thank Lin Guo for her assistance with the graphics. M.H. wishes to thank Don Hunt for giving him time off from his regular duties to write the manuscript.

References

[1] W. Kaye, *Anal. Chem.*, 34 (1962) 287.
[2] D.L. Van Engelen, A.K. Adams and L.C. Thomas, *J. Chromatogr.*, 331 (1985) 77.
[3] D.L. Van Engelen, L.C. Thomas and E.H. Piepmeier, *J. Chromatogr.*, 405 (1987) 191.
[4] M. Novotny, F.J. Schwende, M.J. Hartigan and J.E. Purcell, *Anal. Chem.*, 52 (1980) 736.
[5] M. Kube, M. Tierney and D.M. Lubman, *Anal. Chim. Acta*, 171 (1985), 375.
[6] V. Lagesson and J.M. Newman, *J. High Resolut. Chromatogr. Chromatogr. Commun.*, 11 (1988) 577.
[7] V. Lagesson and J.M. Newman, *Anal. Chem.*, 61 (1989) 1249.
[8] D.M. Lisitsyn and V.I. Gorshkov, *Vses. Nauchno-Issled. Geologorazved. Neft. Inst.*, 246 (1983) 28.
[9] T. Ding and Z. Yan, *Fenxi Huaxue*, 13 (1985) 310.
[10] D.J. Bornhop and J.G. Wangsgaard, *J. High Resolut. Chromatogr.*, 14 (1991) 344.
[11] D.J. Bornhop, L. Hlousek, M. Hackett, H. Wang and G.C. Miller, *Rev. Sci. Instrum.*, 63 (1992) 191.
[12] C.F. Poole and S.A. Schuette, *Contemporary Practice of Chromatography*, Elsevier, Amsterdam, 1986, Ch. 5.
[13] *Linear UVIS-206 Multiple Wavelength Detector*, Instruction Manual, Linear Instruments, Reno, NV, 1989, Ch. 7.
[14] T.G. Hartman, J. Lech, V.G. Saltamach and R.T. Rosen, *Mass Spec Source*, 13 (1990) 31.
[15] H.V. Malmstadt, C.G. Enke and S.R. Crouch, *Electronics and Instrumentation For Scientists*, Benjamin Cummings, Reading, 4th ed., 1981, Ch. 6.
[16] R.M. Silverstein, G.C. Bassler and T.C. Morrill, *Spectrometric Identification of Organic Compounds*, Wiley, New York, 4th ed., 1981, Ch. 6.
[17] P.R. Bevington, *Data Reduction and Error Analysis for the Physical Sciences*, McGraw-Hill, New York, 1969, p. 257.
[18] J.C. Miller and J.N. Miller, *Statistics for Analytical Chemistry*, Ellis Horwood, New York, 3rd ed., 1993, Ch. 5.
[19] M. Hackett, *Thesis*, University of Nevada, Reno, NV, 1991.
[20] E. Wieteska, in T. Nowicka-Jankowska, K. Gorczyńska, A. Michalik and E. Wieteska, *Analytical Visible and Ultraviolet Spectrometry (Wilson and Wilson's Comprehensive Analytical Chemistry*, edited by G. Svehla, Vol. 29), Elsevier, Amsterdam, 1986, Ch. 3.
[21] K. Gorczyńska, in T. Nowicka-Jankowska, K. Gorczyńska, A. Michalik and E. Wieteska, *Analytical Visible and Ultraviolet Spectrometry (Wilson and Wilson's Comprehensive Analytical Chemistry*, edited by G. Svehla, Vol. 29), Elsevier, Amsterdam, 1986, Ch. 9.
[22] S.J. Hein, E.H. Piepmeier and L.C. Thomas, *J. Chromatogr.*, 557 (1991) 39.

[23] M.D. Erickson, *Analytical Chemistry of PCBs*, Butterworth, Boston, MA, 1986, Ch. 2.
[24] E.S. Stern and C.J. Timmons, *Electronic Absorption Spectroscopy in Organic Chemistry*, Edward Arnold, London, 1970, Ch 6.
[25] C.J. Kirchmer, in L.A. Currie (Editor), *Detection in Analytical Chemistry (ACS Symposium Series*, No. 361), American Chemical Society, Washington, DC, 1988, Ch. 4.
[26] C.F. Poole and S.A. Schuette, *Contemporary Practice of Chromatography*, Elsevier, Amsterdam, 1986, Ch. 1.
[27] K. Grob, *Classical Split and Splitless Injection in Capillary GC*, Hüthig, Heidelberg, 2nd ed., 1988.
[28] R. Gale, USFWS, Columbia, MO, personal communication.
[29] M.J. Kamlet (Editor), *Organic Electronic Spectral Data, Vol. 1, 1946–1952*, Interscience, New York, 1960, p. 203.